Auxiliary free space optical communication project to ensure continuous transfer of data for DAG the 4m telescope

Onur Keskin*[a], Cahit Yesilyaprak[b], Sinan Kaan Yerli[c]
[a] FMV Işık University, Department of Mechanical Engineering, Istanbul/Turkey; [b] Atatürk University, Science Faculty, Department of Astronomy and Astrophysics, Erzurum/Turkey; [c] Orta Doğu Teknik Üniversitesi (METU), Physics Department, Ankara/Turkey.

ABSTRACT

The continuity of the amount of data that the 4m DAG (Eastern Anatolia Observatory in Turkish) telescope will produce and transfer to Ataturk University is critical not to jeopardize the science programs. Though the fiber optics and radio link infrastructures are in place, these systems are still volatile against earthquakes, and possible excavation damages. Thus the 4m DAG telescope will be equipped with a free space optical communication system to ensure the continuity of the data transfer as a backup system. In order to cope with the disturbances introduced by the atmospheric turbulence, the transceiver FSO system will be equipped with a wavefront corrector. In this paper, the Cassegrain optical design, and working principle of this system as well as expected performance analyses will be presented.

Keywords: FSO Communication, Laser, Atmospheric compensation

1. INTRODUCTION

The beginning of the 21st Century gave rise to an era of information and globalization in the world, where secure communication and protection of sensitive data is of utmost importance. The photons can propagate in two media namely the optical fibers and free-space. Almost all commercial schemes use optical fiber as a communication channel. A reason for that may be found in the relative simplicity in handling a fiber based channel instead of a free-space one. In free-space applications, nontrivial impairments arising from molecular aerosol and turbulence effects over atmospheric paths cause a series of distortion effects (beam spreading, beam wander, and intensity fluctuations) in optical waves that are propagating through. This distortion can be compensated by means of an alternative approach called adaptive optics (AO) systems. In this architecture, the optical system becomes smart, it adapts itself to the aberrations of the transmission medium and compensates for them. This is not possible with classical (static) optical systems.

DAG auxiliary free space optical communication system will use a model based and experimentally evaluated AO based optical communication scheme. The good agreements between the numerical and experimental evaluation of data transfer between Alice (transmitter) and Bob (receiver) will ensure the successful implementation of the methodology.

One of the challenges in free-space communication systems arises from the temporal and field-dependent evolution of the atmospheric turbulence. The angle of arrival methodology will be used to define the mean slope (the first derivative) of the turbulent wavefront. This will enable us to investigate the agreement of the spatio-temporal properties of the generated turbulence with Kolmogorov and Von Karman theories. Furthermore, the turbulence emulator will generate the optical effects of the atmospheric turbulence to the wavefront that will used to test the AO control system.

To understand the importance of this project one has to realize that the performance of an optical communication link is limited by turbulence induced disruptions arising from the refractive index inhomogeneities, and noise level of system electronics. Data encoding techniques can be used to eliminate the effect of the noise level of the employed electronics. But the effect of atmospheric signal fading can't be recovered without sacrificing the communication system's data throughput rate. Consequently, during data transfer with free-space systems, the constant variation of atmospheric turbulence has to be compensated via, for instance, AO systems, in order to get accurate results across the communication field. The research goal of this project can then be defined as an accurate estimation of the optical

* O.Keskin: onur.keskin@isikuni.edu.tr

Advances in Optical and Mechanical Technologies for Telescopes and Instrumentation II,
edited by Ramón Navarro, James H. Burge, Proc. of SPIE Vol. 9912, 991273
 · doi: 10.1117/12.2234388

properties of atmospheric turbulence, compensation for these effects using AO systems that will be used in the next-generation free-space information and processing systems.

2. RESEARCH METHODOLOGY

Refractive index inhomogeneities of the turbulent air cause wavefront distortions in optical waves propagating through the atmosphere. AO systems use real-time wavefront control schemes to compensate for distortions. However, AO technologies, currently used in astronomical applications, need to be adjusted to the requirements of free-space optical communications systems. For example, astronomical observatory sites are selected specifically in view of low turbulences, and observations are usually made of objects at higher elevation angles. In contrast, free-space communication scenarios are typically characterized by much stronger turbulence results near ground.

In classical optical communication systems, generally, a divergent beam at Alice is employed to generate an oversized beam footprint at Bob to rule out the necessity for real-time tracking. Though, the performance of an optical communication link is limited by turbulence induced disruptions arising from the refractive index inhomogeneities, and noise level of employed electronics, the noise level of the electronics can be compensated by data encoding techniques, but atmospheric signal fading can not be recovered without sacrificing the communication system's data throughput rate. A solution to this problem is the use of AO systems. It must be noted that the signal fading does not severely limit the performance of communication systems. Regardless of this difference, the use of AO systems in free-space communication can improve signal stability and enhance overall link transmittance.

A conventional adaptive optics system, regardless whether it is used for astronomical imaging or for laser beam propagation, consists of three principal components: (i) a wavefront sensor to detect the optical disturbance; (ii) a tip/tilt (TT) and/or deformable mirror (DM) to correct for the optical disturbance; and (iii) actuator command electronics to acquire the sensor information, compute the required corrective action, and to control the tip/tilt and/or deformable mirror. In free-space communication systems AO can be used in different architectures; one approach can be the use of AO at the receiver end of the communication link: In this scheme, a tip/tilt mirror can be employed to adjust the position offsets of the incoming distorted wavefront by counteracting the apparent motion of the beam. It must be noted that atmospheric tip and tilt represent the lowest order aberrations and are responsible for almost 87% of the Kolmogorov's theory of optical turbulence. Tip/tilt correction is usually sufficient if the detector area is large enough not to clip the focal spot. But if the received beam is to be coupled into an optical fiber, the compensation of higher order aberrations is still required, and can be achieved by means of a deformable mirror.

To increase the total power of light collected on the receiver end of the communication scheme, an AO based transmitter is also required as the receiver only compensates for the present distortions on the incoming beam entering receiver telescope's aperture. This adaptive transmitter can be used to precompensate the transmitted wavefront against turbulence induced beam spreading. An AO based transmitter can be realized in two ways; (i) the feedback data, on the sensed wavefront distortions, can be acquired from Bob and sent to Alice to optimize the precompensation of the transmitted beam. The feedback signal's intermission due to the propagation time represents a fundamental constraint to this approach, and limits its practicability to shorter link distances; (ii) an auxiliary laser, generated from Bob, can be employed to measure the level of atmospheric distortion on the light propagating through stations. The controller's role is to interpret the wavefront data, and to determine what adjustments are necessary to the angle adjustments of the tip/tilt mirror and to the physical shape of the deformable mirror in order to compensate for the present aberrations in the light path. The control system enhances the beacon's beam quality in the transmitter end and the beam is sent back to the receiver using the same AO elements. According to Kolmogorov's theory of optical turbulence, the refractive index fluctuations are homogeneous and isotropic, and are assumed to have a Gaussian random distribution. The round trip propagation (Bob-Alice-Bob) must be faster than the time scale of atmospheric turbulence variations (~ 1-2 ms). Within this time frame the atmospheric turbulence is assumed to be frozen (Taylor hypothesis) in the entrance pupil of the transmitting telescope. The correction of the incoming beam at Alice then offers the optimal precompensation in direction to Bob.

The atmosphere has a high transmission window at a wavelength of around 770nm. High efficiency SiAPDs (Avalanche photodiode with detection efficiency as high as 65% and low noise) can be used at 770nm of wavelength for this scheme. Furthermore, the atmosphere is weakly scattered and it is isotropic. Thus, it will not alter the polarization state of a photon.

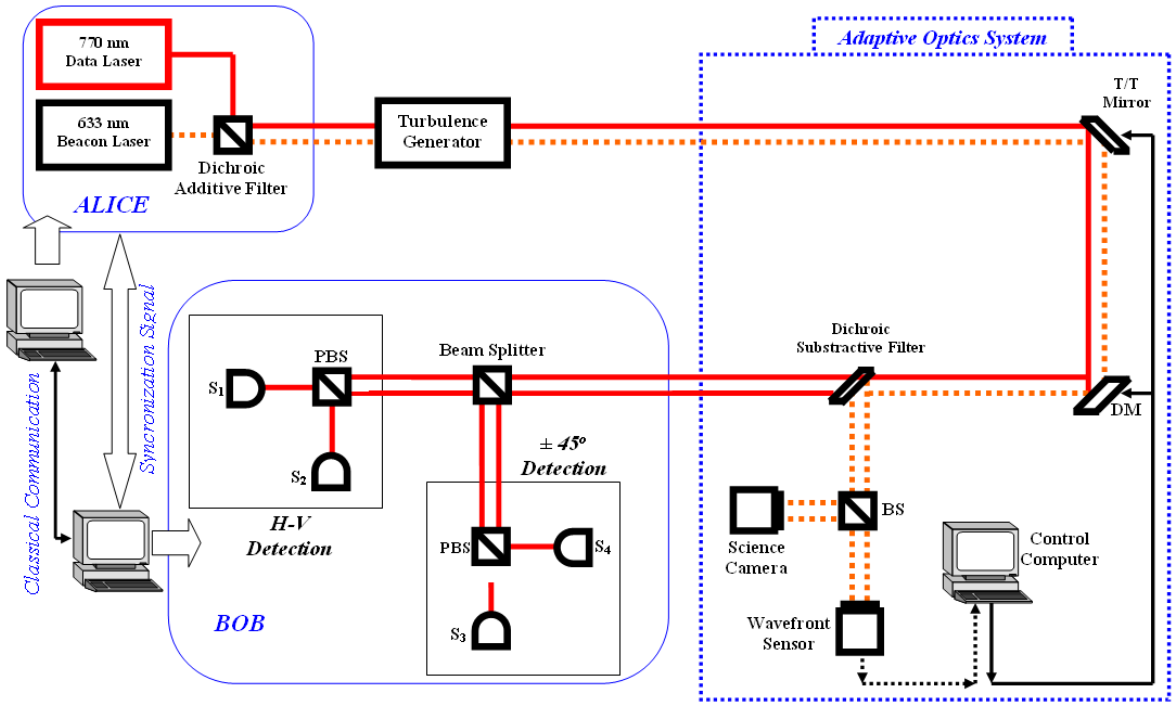

Figure 1: The FSO-AO scheme, where Alice: Transmitter, Bob: Receiver, S: SiAPD, BS: Beam splitter, DM: Deformable mirror, PBS: Polarizing beam splitter, H-V: Defined states

2.1 The Test Bed

In the AO part of the test bed, a collimated point light source, goes through the atmospheric emulator [1] and becomes aberrated. The degree of distortion of the wavefront is detected by the SH WFS. The purpose of the AO system is to compensate to the distortions. The TT mirror adjusts the angle-of-arrival variations (i.e. tip/tilt) by counteracting the motion of the light. The DM uses a grid of actuators to oppose to the shape of the distorted wavefront. In the wavefront-compensation, the commands of mirrors are determined by the controller, which uses the Shack Hartmann Wavefront Sensor (SH WFS) measurements. During this closed-loop operation, the WFS measures only the residual wavefront error. The process operates in real time to compensate for the constant variations of atmospheric turbulence. The major components of the system will be described in the following sub-sections.

2.2 Tip/tilt Mirror

Tip/tilt mirror (adjusts the position offsets of the incoming distorted wavefront. Atmospheric tip and tilt is responsible for almost 87% of the Kolmogorov phase variance [2]. The compensation of tip and tilt modes also assists in reducing the required stroke of the DM. This is also called a first-order correction involving the removal of the random displacements of the image, also referred to as tip-tilt correction. Tyler demonstrated that the bandwidth required for tip-tilt correction is about nine times lower than that required for complete atmospheric compensation [3]. The main effect of optical turbulence on a beam of diameter D is the creation of phase aberrations, for which the aberration variances can be shown to be proportional to the ratio of pupil diameter to the Fried coherence length [4], $(D/r_0)^{5/3}$:

$$\sigma_1^2 \text{ modes removed} = 1.0299\left(\frac{D}{r_0}\right)^{5/3} \quad (1)$$

The wavefront variance terms for the tip mode can be expressed as:

$$\sigma_2^2 \text{ modes (tip) removed} = 0.582\left(\frac{D}{r_0}\right)^{5/3} \quad (2)$$

The wavefront variance terms for the tilt mode can be expressed as:

$$\sigma_3^2 \text{ modes removed} = 0.134\left(\frac{D}{r_0}\right)^{5/3} \quad (3)$$

The TT mirror axes of rotation are defined in **Figure 2**a. The TT mirror uses multilayer piezo-actuators: piezoelectric materials change dimension when an electric field is applied; they are shown in **Figure 2**b. A multilayer piezo-actuator is a stack of thin films of zirconium titanate electrically connected in parallel. The thinner the film, the lower the voltage required for the maximum expansion of the multilayer stack.

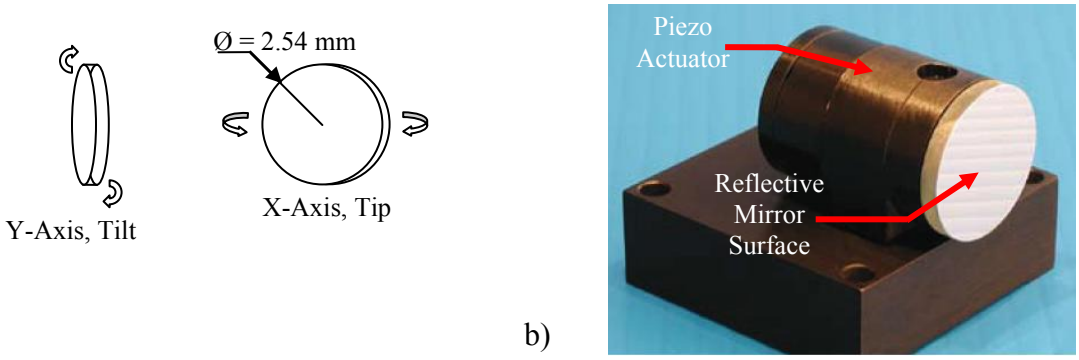

Figure 2: (a) Configuration of the TT mirror; (b) multilayer piezo-actuator, the thin film layers of zirconium titanate are separated by conducting layers.

2.3 Deformable Mirror

Figure 3 illustrates the working principle of the continuous deformable mirror. The actuator membrane serves as the upper electrode of a parallel plate capacitor. The stationary layer on the bottom actuator electrode serves as the second electrode of the capacitor. When a voltage difference is applied between the lower electrode and the grounded upper electrode, the actuator membrane deflects downwards/upwards. The attachment post and mirror surface are correspondingly deflected. In order to provide the high surface quality of the DM, a chemo-mechanical polishing process is followed up with a gold coating process. This has improved the reflectivity without introducing a significant amount of stress in the mirror membrane.

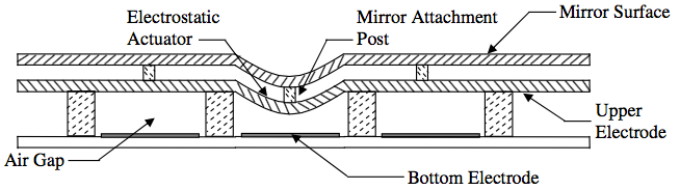

Figure 3: Deformation principle of the continuous mirror.

Figure 4a illustrates the configuration of the DM containing 12 x 12 actuators. The actuators on the border of the DM are not used for correction. This reduces the number of actuators to 10 x 10. It must be noted that the DM is conjugated to the entrance pupil of the telescope. The entrance pupil emulates the telescope's aperture. Therefore, the physical diameter of the light is limited by the telescope's aperture.

The wavefront variance terms for these DM modes can then be expressed as:

$$\sigma^2_{80\,DM\ modes\ removed} = 0.2944 N_{Zernike}^{-\sqrt{3}/2} \left(\frac{D}{r_0}\right)^{5/3} \tag{4}$$

where N is the number of Woofer modes. Influence functions can be defined as a map of the physical deformations on the DM surface under a given voltage. One poked actuator influences its neighbour actuators; and is shown for a single actuator in **Figure 4**b. The reflective surface of the mirror is flat to within 1 nm rms; this can be seen in **Figure 4**c. **Figure 4**d illustrates the DM surface deformation in a downward direction, the mirror provides 1.5 µm of maximum stroke.

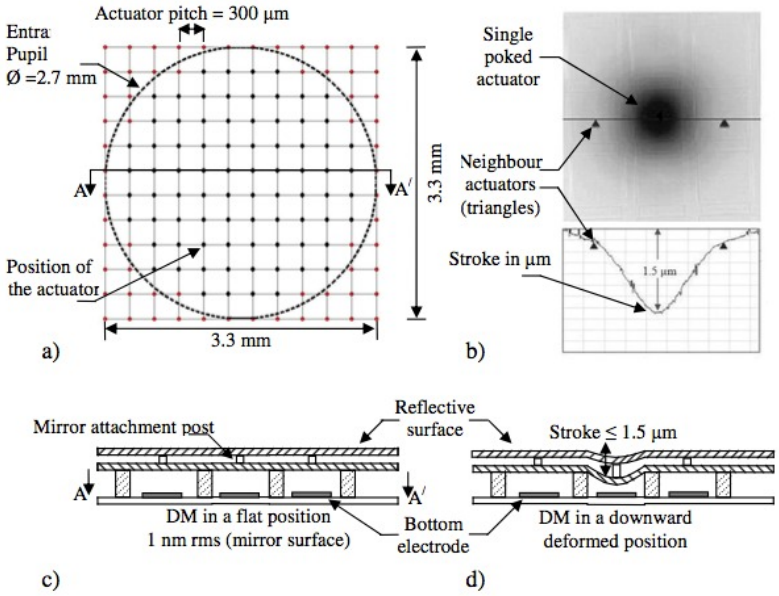

Figure 4: Design and layout of actuators in the DM: (a) the configuration of actuators; (b) illustration of an influence function; (c) reflective surface without deflection; (d) downward position of the mirror

2.4 Shack-Hartmann Wavefront Sensor

The Shack-Hartmann wavefront sensor placed on the test-bed (SH WFS) is made of 132 x 132 square lenslets with a pitch of 188 µm and 8 mm focal length. The registration is critical for the stability of the control system. On the numerical evaluations, a lenslet subset is matched to the DM actuators [5]; this can be seen in **Figure 5**. The DM is registered to the vertices of these lenslets.

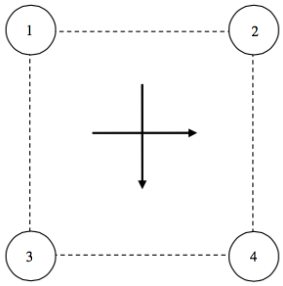

Figure 5: Fried geometry; the numbered small circles represent actuator positions and the dotted large square represents one of the square sub-apertures with the orthogonal slope measurements represented by the arrows.

In the design and layout of SH WFS used the 9 x 9 portion of the SH WFS used. The lenslet is formed from a sheet of micro-lenses, also termed a lenslet array, and is placed in a plane conjugate to the pupil. Each lenslet is a sub-aperture. The sub-apertures intercept the light from a section of the full pupil image, and form an image of the source at the lenslet focal plane. Within this portion, the WFS is conjugated to the pupil, as well; only the section corresponding to the entrance pupil will be illuminated. A quad-cell, is placed at the image of each lenslet, representing a reference plane wave. The intensity of the light is equal in each quadrant. Alternatively, in case of a disturbed wavefront, the aberrations on the incoming wavefront across a lenslet sub-aperture will cause the focused spot to displace an amount proportional to the local wavefront slope. From the angle of arrival calculation, the centroid movement can be calculated. The centroid tracking in x- and y-coordinates can be determined from the intensities in those quadrants, where the signal from one quadrant (i) is increased, while that from the other three quadrants is reduced.

In the numerical evaluations, centroid estimation is accomplished using a center-of-gravity calculation [6]:

$$cent_x = \frac{\sum_{i,j} x_{i,j} I_{i,j}}{\sum_{i,i} I_{i,i}} \qquad and \qquad cent_y = \frac{\sum_{i,j} y_{i,j} I_{i,j}}{\sum_{i,i} I_{i,i}} \tag{5}$$

3. NUMERICAL RESULTS AND CONCLUSIONS

As the communication set-up is still on the progress, the numerical modeling of the AO performance is performed via PSF reconstruction. The adapted methodology [7][8] has the advantage of a PSF estimation based on the data measured synchronously with the observation.

During an AO correction, the SH WFS will provide a measurement of the phase of the residual wavefront error $\varphi(\vec{r},t)$ at each acquisition. From these measurements the average structure function, $\overline{D}_{\varphi_\varepsilon}(\vec{\rho})$ of this phase can be calculated.

$$\overline{D}_{\varphi_\varepsilon}(\vec{\rho}) = \left\langle \left| \varphi_\varepsilon(\vec{r},t) - \varphi_\varepsilon(\vec{r}+\vec{\rho},t) \right|^2 \right\rangle \tag{6}$$

where vectors $\vec{r}$ and $\vec{\rho}$ represent two dimensional positions and separations in the pupil plane. SH WFS measurements obtained from the long exposure are limited to the DM's spatial cutting frequency; therefore, only the DM component of the phase variations can be measured. The residual phase can be decomposed into two components; φP the parallel component of the residual phase (phase projected onto the mirror) and φO the orthogonal component of the phase (residual phase that is not corrected by the mirror).

$$\varphi_{total} = \varphi_P + \varphi_O \tag{7}$$

Note that φO is not corrected by the system, and it will be estimated from the Kolmogorov model of the turbulence. To reconstruct the PSF from a single DM AO system first the OTF of the system must be computed:

$$OTF_{AO}(\vec{\rho},\lambda) = \exp\left[-\frac{1}{2}\left(D_{\varphi_P}(\vec{\rho}) + D_{\varphi_O}(\vec{\rho}) \right) \right] \tag{8}$$

and,

$$OTF_{Total}(\vec{\rho},\lambda) = OTF_{AO}(\vec{\rho},\lambda).OTF_{TEL}(\vec{\rho},\lambda) \tag{9}$$

where OTF_{TEL} is the residual from the AO correction containing the diffraction patterns from the telescope and uncorrected static aberrations, and OTF_{AO} contains the contribution of the turbulence. The PSF can then be calculated by taking the inverse Fourier transform of the OTF_{Total}.

The structure function of the OTF_{TEL} and OTF_{AO} can be expressed as:

$$D_{\varphi_P}(\vec{r},\vec{\rho}) = \left\langle \left| \varphi_P(\vec{r},t) - \varphi_P(\vec{r}+\vec{\rho},t) \right|^2 \right\rangle \text{,and } D_{\varphi_O}(\vec{r},\vec{\rho}) = \left\langle \left| \varphi_O(\vec{r},t) - \varphi_O(\vec{r}+\vec{\rho},t) \right|^2 \right\rangle \tag{10}$$

If one can substitute $\varphi_P(\vec{r},\vec{\rho})$ with its modal decomposition of the mirror modes:

$$\varphi_P(\vec{r},t) = \sum_{i=1}^{N} \varepsilon_i(t) M_i(\vec{r}) \tag{11}$$

where N is the modes of the mirror, the structure function of the DM of the OTF_{TEL} and OTF_{AO} becomes:

$$D_{\varphi_P}(\vec{\rho}) = \sum_{i=1}^{N}\sum_{j=1}^{N} \left\langle \varepsilon_i \varepsilon_j \right\rangle U_{ij}(\vec{\rho}) \tag{12}$$

where $U_{ij}(\vec{\rho})$ function depends only on the geometry of the system, P the pupil function

$$U_{ij}(\vec{\rho}) = \frac{\int P(\vec{r})P(\vec{r}+\vec{\rho})\left[M_i(\vec{r}) - M_i(\vec{r}+\vec{\rho})\right]\left[M_j(\vec{r}) - M_j(\vec{r}+\vec{\rho})\right]d\vec{r}}{\int P(\vec{r})P(\vec{r}+\vec{\rho})d\vec{r}} \tag{13}$$

The <εiεj> is the covariance matrix of the mirror modes error commands, related to WFS measurements covariance matrix <wiwj> and the aliased orthogonal modes covariance matrix <αiαj>.

$$\left\langle \varepsilon_i \varepsilon_j \right\rangle = D^+ \left\langle w_i w_j \right\rangle (D^+)^t + \left\langle \alpha_i \alpha_j \right\rangle \tag{14}$$

where D+ is the command matrix gathered from the SH WFS measurements. The structure function of the OTF_{AO} can be calculated numerically using a Monte-Carlo model of the AO system. This can be done by removing the mirror modes out of each phase screen and then computing the average of the structure function for the corrected phase screens [9].

The inputs for the reconstruction of the PSF from the system modeling can be summarized as: (i) the residual wavefront error data from the synchronous SH WFS measurements, (ii) the command matrix of the control loop, and (iii) the system's geometry. The computed parameters are: (i) the commands projected onto the mirror modes, (ii) the parallel and orthogonal structure function of the atmospheric turbulence, (iii) the covariance matrix of the WFS, and (iv) the OTF of the telescope.

The plot (Figure 6) represents a single one-dimensional cut through the OTFs shown above. The plot represents a symmetrical cut to distinguish discrepancies between the OTF_{TEL}, OTF obtained from the science camera, and the reconstructed OTF.

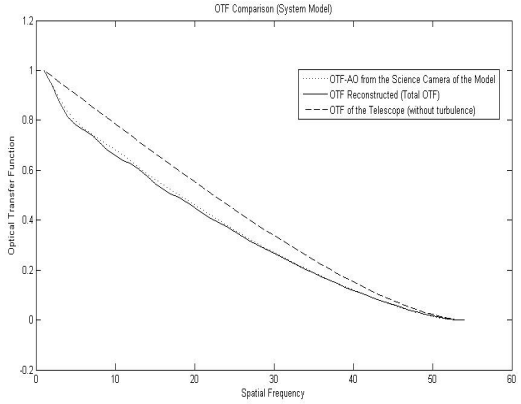

Figure 6. Reconstructed OTFs (Numerical)

In Figure 6, the comparisons between the numerical OTFs are represented. The agreement between the calculated optical transfer functions and the ones obtained from the AO correction can be clearly seen. It must be added that these preliminary results do not include the aliasing error effect.

FUTURE WORK

The numerical results will be further investigated on the experimental test bench while both on the numerical model and the experimental model aliasing error will be observed. The accomplishments of the implementation will lead to the establishment of baseline theoretical and experimental performance. This knowledge will be used to improve the outcome of the FSO system to be used as an auxiliary system for data transfer between DAG telescope and Ataturk University in the line of sight of 12 km distance.

ACKNOWLEDGMENTS

Authors would like to thank FMV Işık University, Istanbul/Turkey; Atatürk University, Erzurum/Turkey (Project No: 2011K120230, 2016K121140); Orta Doğu Teknik Üniversitesi, Ankara/Turkey (Project No: 2016K121380); Republic of Turkey, Ministry of Development; Atatürk University, Erzurum/Turkey, Astrophysics Research and Application Center (ATASAM), Erzurum/Turkey; FMV Işık University, Center of Optomechatronics Application and Research (OPAM), Istanbul/Turkey; for their support throughout the DAG project.

REFERENCES

[1] O. Keskin, L. Jolissaint, C. Bradley, "Hot-air optical turbulence generator for the testing of adaptive optics systems: principles and characterization," *Applied Optics*, Vol. 45, Issue 20, pp. 4888-4897, (2006).

[2] R. J. Noll, "Zernike polynomials and atmospheric turbulence," *J. Opt. Soc. Am*. 66, 207–211, (1976).

[3] G. A. Tyler, "Bandwidth considerations for tracking through turbulence," *Journal of the Optical Society of America,* 11:358–367, (1994).

[4] D. L. Fried, "Optical resolution through a randomly inhomogeneous medium for very long and very short exposures," *J. Opt. Soc. Am.* **56,** 1372–1379, (1966).

[5] D. L. Fried, "Statistics of a Geometric Representation of Wavefront Distortion," *Journal of the Optical Society of America*, 55:1427–1435, (1965).

[6] M. Kasper, D. Looze, S. Hippler, R. Davies, and A. Glinderman, "Increasing the Sensitivity of a Shack-Hartmann sensor," *In Canterbury Conference on Wavefront Sensing and its Applications*, (1999).

[7] J.P. Veran, F.Rigaut, H. Maiter, and D. Rouan, "Estimation of the adaptive optics long exposure point spread function using control loop data," *J. Opt. Soc. Am.* A, 14, (1997).

[8] L. Jolissaint, J.P. Veran, "OPERA, an automatic PSF reconstruction software for Shack-Hartmann AO systems: application to Altair," *Proc. SPIE*, volume 5490, 151-163, (2004).

[9] O. Keskin, R. Conan, P. Hampton, C. Bradley, "Derivation and Experimental Evaluation of a Point Spread Function from a Dual Deformable Mirror Adaptive Optics System," Optical Engineering, Vol.47, No. 4, p. 046601, (2008).